Fringe-tracking experiments at the IOTA interferometer

S. Morel[a], W. A. Traub[b], J. D. Bregman[c], R. Mah[c], and E. Wilson[c]

[a]Smithsonian Astrophysical Observatory - F. L. Whipple Observatory
670 Mount-Hopkins Road, Amado, AZ 85645, USA

[b]Smithsonian Astrophysical Observatory - Center for Astrophysics
60 Garden Street, Cambridge, MA 02138, USA

[c]NASA - Ames Research Center, MS 245-6
Moffet-Field, CA 94035, USA

ABSTRACT

The first tests of an infrared fringe-tracker prototype for the IOTA interferometer (Mount-Hopkins, Arizona) were carried out during 1999. The aim of this real-time system is to minimize the optical path difference (OPD) fluctuations between the two beams such that interference fringes (obtained in J, K, or L band) can always be observed within the "scan window" given by the instrument. After an introduction of the employed technology (hardware and software), we present results obtained from star observations. Finally, we discuss the possibility of improving the fringe-tracker by prediction of the OPD, using statistical properties of its fluctuations. The improvement of the fringe-tracker already existing for the FLUOR recombiner is discussed as well.

Keywords: fringe-tracking, coherencing, infrared detectors, precision positioning, prediction.

1. INTRODUCTION

A two-aperture stellar optical interferometer is always subject, while being operated, to variations of the optical path difference (OPD) between the two light beams coming from its telescopes. One of the OPD variation components is a deterministic signal related to the Earth's rotation. It is compensated by moving an optical delay line (ODL) according to a pointing model given by the declination of the observed object and its hour angle. The other components are random and are caused by atmospheric turbulence ("differential piston" mode of the turbulence), mechanical constraints, vibrations, and errors in the pointing model. Interference fringes are observable within an OPD interval roughly equal to the coherence length defined by $L_c = \bar{\lambda}^2/\Delta\lambda$, where $\bar{\lambda}$ is the mean filter wavelength and $\Delta\lambda$ is the spectral bandpass. Because of the random fluctuations in the OPD, during an observation the OPD is scanned on either side of the expected null-OPD point by a piezo-electric controlled mirror.

The aim of fringe-tracking is to perform a real-time correction of the length difference between the actual null-OPD position and the expected null-OPD position, in order to keep the fringes centered in the observing window. This difference is computed from the acquired fringe signal and is used to control an optical delaying device. In order to not "share the photons", the fringe-tracker uses the same data as for producing the "scientific" fringes, which are acquired for measuring source visibility points from the fringe contrast (imaging interferometry) or external delay (in case of astrometry by interferometry). However, in some cases, it may be useful to have separate recombiners for acquisition and tracking[1].

Further author information:

S.M.: E-mail: smorel@cfa.harvard.edu. Fax: 1 520 670 5751
W.A.T.: E-mail: wtraub@cfa.harvard.edu. Fax: 1 617 495 7105
J.D.B.: E-mail: jbregman@mail.arc.nasa.gov
R.M.: E-mail: rmah@mail.arc.nasa.gov
E.W.: E-mail: ed.wilson@ibm.net

Although it is possible to manually track the fringes (see part 3), significant fringe acquisition improvements are expected from an automatic fringe-tracker. The implementation of a fringe-tracker depends on the way fringes are acquired. With channeled spectra (for small apertures) or dispersed fringes (for apertures larger than Fried's parameter r_0) configurations, one can track fringes by respectively group-delay tracking[2] (GDT) or real-time active fringe tracking[3] (RAFT). This is done at visible wavelengths using photon-counting detectors. However, no photon-counting technology currently exists for the infrared: the fringe signal-to-noise ratio decreases with the number of pixels of the detector. The signal should be therefore "concentrated" on a minimal number of pixels. The classical "white-fringe" set-up is then employed (Fig. 1). The two beams are recombined by a beamsplitter. Fringes are acquired by linearly modulating (by a sawtooth signal ideally) the pathlength of one of the beams upstream from the recombination. Intensities of the recombined beams evolve therefore temporally as an interference fringe pattern. Due to reflections on the beamsplitter, there is a π phase-shift between the two interferometric signals obtained.

The pathlength scanned depends on the detector performances and is usually equal to a few coherence lengths. For a white-fringe set-up, one can perform "cophasing" in order to "freeze" fringes moved by atmospheric differential piston[4]. However, a very good fringe SNR is necessary for this technique. A less demanding way to perform fringe-tracking is called "coherencing": the OPD is corrected so that the fringes remain within the "observing window" defined by the scan length. Group-delay tracking and RAFT may be regarded as coherencing techniques. For any set-up, the OPD correction rate is between 0.2 Hz and 10 Hz. The duration of a cycle is therefore longer than the atmospheric τ_0.

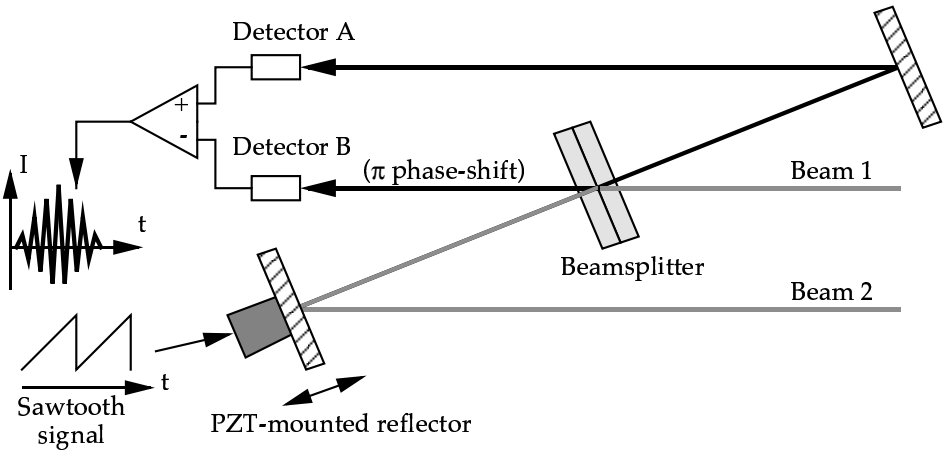

Figure 1. Schematic of a recombination table based on a beamsplitter, as it is employed at IOTA for fringe acquisition.

2. COHERENCING ALGORITHM

With a white-fringe set-up, the two interferometric signals resulting from a scan are subtracted to yield an interferogram. For each interferogram (or fringe packet) acquired, the computer performing fringe-tracking finds the null-OPD point and computes the offset to apply to the delaying device, in order to bring the null-OPD point to the center of the observing window (i.e., half-way along the scan length).

For IOTA (see part 3), a fringe packet scan consists of 256 temporally sampled points. Each value is a 16-bit integer. We use the following algorithm to find the null-OPD point in a fringe packet:

1) The photometric variations are removed by subtracting the local mean from each value of the fringe packet (computed from the values of the 20 points closest to a given point). An FFT bandpass filter can be used instead, and gives satisfactory results.
2) Any negative values in the scan are multiplied by -1 (equivalent to a rectifier bridge).
3) All the values that are not local maxima are set to zero.
4) Linear segments are interpolated between each pair of non-zero points (corresponding to the fringe peaks in the interferogram).

5) The resulting signal is smoothed by a "schematized" coherence envelope given by flat-top functions representing the main lobe and two sidelobes. The location of the maximum value in the signal resulting from the previous operation gives the null-OPD point.

These steps are illustrated in Fig. 2. This algorithm is actually a simplified version of one we developed that included phase measurement. The algorithm was first tested in the MatLab language using recorded interferograms, and showed good robustness to noise. Tests were also done using simulated interferograms: the RMS error on the null-OPD point found is never larger than 20 points. With the IOTA fringe acquisition system (see part 3), this corresponds to an error on the estimated null-OPD point of 8 μm, very good for a coherencing system.

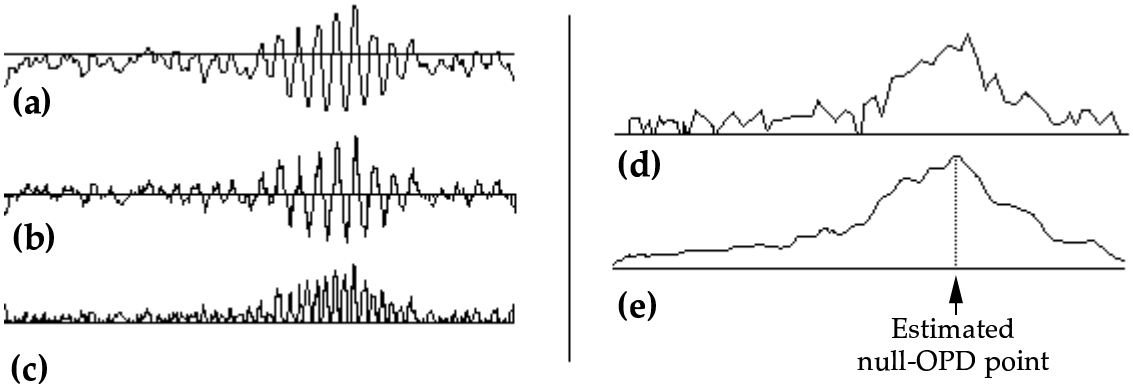

Figure 2. Illustration of the steps of the coherencing algorithm. (a): Interferogram acquired ; (b): signal obtained from this interferogram after step 1 (correction of the photometric variations) ; (c): signal obtained after step 2 (rectification) ; (d): signal obtained after steps 3 and 4 ; (d): signal obtained after step 5 (smoothing). The null-OPD point corresponds to the position of the maximum value in this signal.

3. FRINGE-TRACKER IMPLEMENTATION ON THE IOTA INFRARED TABLE

IOTA can currently use either a single-mode fiber recombiner called FLUOR[5] or a beamsplitter-based recombiner, as described in Fig. 1. For scanning the OPD, a plane mirror is mounted on a piezo-electric transducer (PZT) which is controlled by a triangle signal generated by a low-frequency analog function generator. Our fringe-tracker has been designed for this recombiner only. The detector used for fringe acquisition is based on a 256×256 pixel NICMOS III chip[6]. Only two pixels of this chip are read for acquiring interferometric signals. The maximum rate $f_s = 1/\tau_s$ is 10 interferograms per second, each one being 256 point wide. The NICMOS chip is controlled by signals generated by a 100 MHz Pentium PC which receives the sampled value of the addressed pixel. After processing, these values are sent to a Macintosh Quadra computer for displaying and recording the interferograms.

The delaying device used by IOTA for compensating the OPD due to Earth rotation is the "short ODL". It consists of a dihedral reflector mounted on an Anorad micro-positioning table. This table may be translated within a 2.3 m interval by 10 nm steps thanks to an electric linear motor featuring a laser metrology based position servo-loop. The short ODL is controlled by another Macintosh Quadra. Without fringe-tracking, the operator has to check the position of the interferogram displayed by the first Quadra and manually modify the short ODL position from the second Quadra to keep the fringe packet observable. This operation is difficult when there is significant atmospheric turbulence. Implementing an automatic coherencer fringe-tracking system would therefore significantly improve data acquisition on IOTA.

To implement the fringe-tracker, the algorithm described in part 2 was coded in the C++ language on a temporary Macintosh PowerBook (100 MHz PowerPC CPU). The interferogram acquisition and ODL control programs were modified to communicate with the fringe-tracker computer: each interferogram is sent through the Ethernet local area network (LAN) of IOTA to the fringe-tracker. After having found the null-OPD point in the interferogram, the fringe-tracker computer sends the OPD correction to the ODL control computer which adjusts the short ODL position.

The test of this first version of the IOTA fringe-tracker consisted of observing bright stars such as ι-Aur or β-Gem. Some problems, related to the design of the fringe-tracker were detected. The TCP/IP protocol used for communication between the computers is not suitable for our real-time application involving MacOS computers. Hence, we now use UDP (User Datagram Protocol) which is a socket-based protocol faster and more flexible than TCP/IP, for all the IOTA applications requiring inter-communication by LAN. For example, the long-ODL is managed by a Linux computer located at the north end of the IOTA baseline. This computer is commanded from the Quadra controling ODLs via UDP. A second problem was that at the higher scan rates (10 Hz), the inertia of the short-ODL was too large to allow it to respond to the tracking commands.

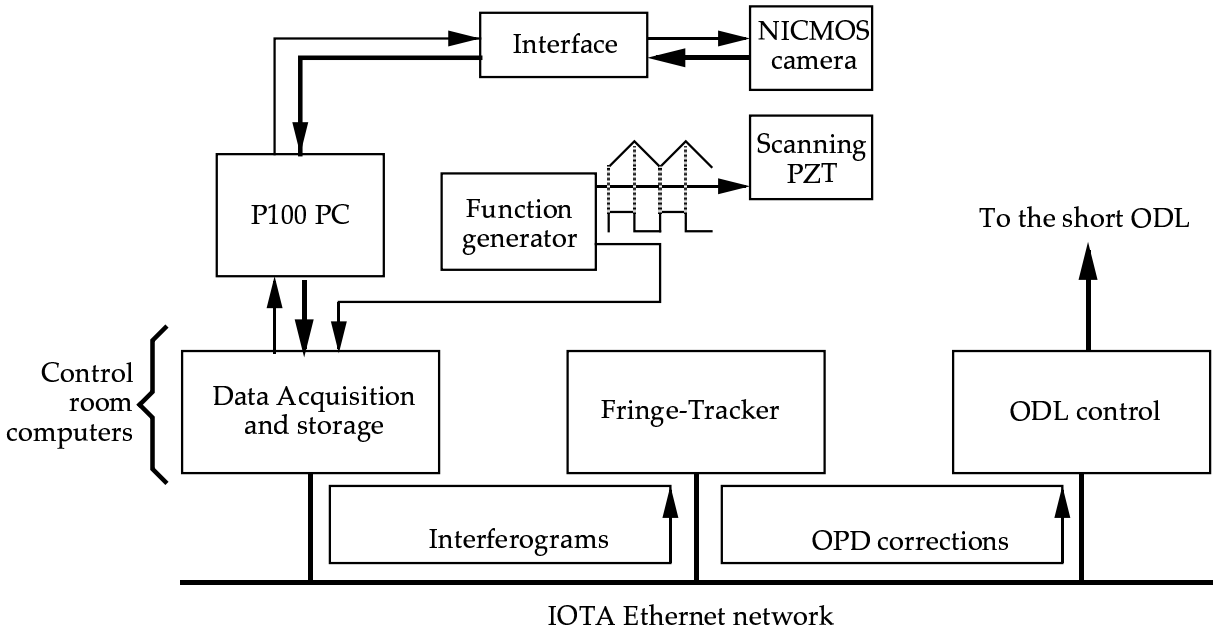

Figure 3. Diagram of the data flow in the fringe-tracking system tested on IOTA.

4. WHAT REMAINS TO BE DONE

4.1 PZT control

The scanning PZT is driven by a Physik Instrumente high-voltage amplifier featuring a function generator programmable by an external computer. All the parameters which control the generated signal are sent through a serial link to the amplifier. It will therefore be possible to reduce the scan range (i.e. slowing down the velocity of the scanning mirror while keeping the same sampling rate) to increase the fringe SNR if the differential piston is not too large. In this case, the high frequency OPD corrections would be directly applied to the scanning PZT by adding an voltage offset to the driving signal. The lower frequency OPD errors, which can exceed the range of the PZT, would be corrected by using the short ODL to bring the PZT back to the middle of its mechanical range (which should correspond to the null-OPD point). Moreover, the duty-cycle of the signal can be modified to increase the efficiency of the acquisition system.

Controlling the PZT requires a device to synchronize the NICMOS acquisition. In the current IOTA control system, acquisitions by the Quadra are triggered by the leading edge of a TTL signal delivered by the external function generator. This TTL signal is synchronized with the triangle signal driving the PZT. For the fringe-tracker using PZT control, we wired an electronic temporal derivator giving a rectangular signal from the signal delivered by the amplifier.

However, the IOTA control system should be soon replaced by a VME chassis with PowerPC boards running under Wind-River's VxWorks, a real-time operating system[7]. Many improvements are expected from this new system which will control siderostat and ODL motion, tip-tilt correction and fringe acquisition. The implementation of a fringe-tracker will be easier thanks to a simplification of the communication between the processes.

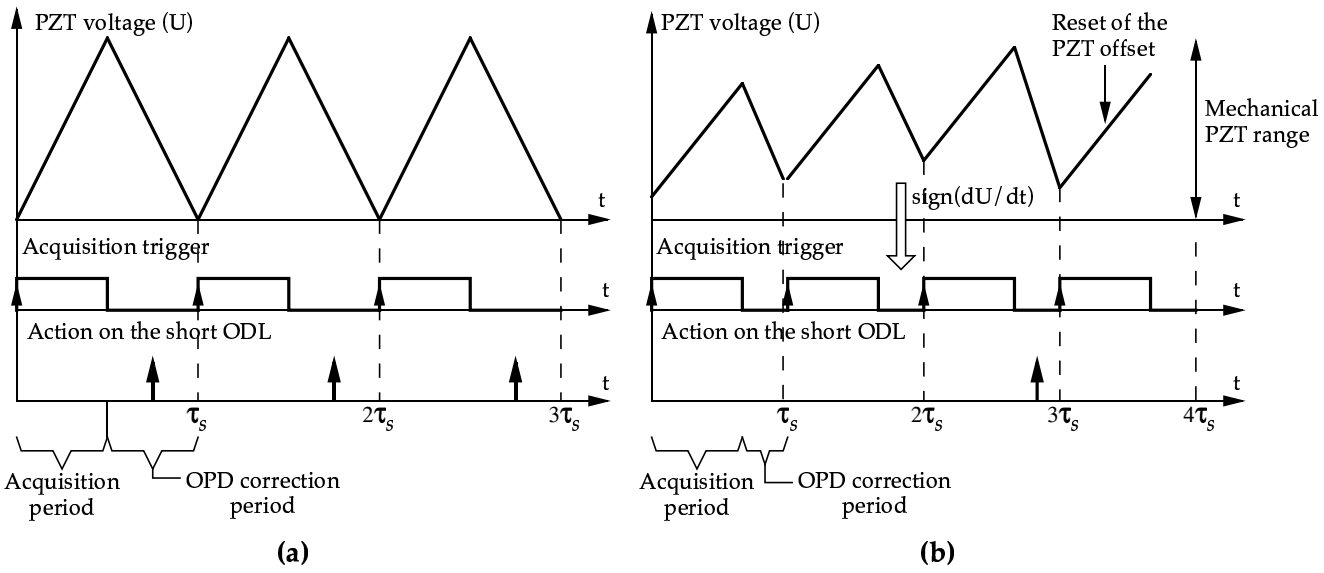

Figure 4. Chronograms of the voltage applied to the scanning PZT, the corresponding TTL signal for triggering NICMOS acquisitions, and the OPD correction on the short optical delay-line. (a): current situation ; (b): future system with PZT control by the fringe-tracker.

4.2 Prediction of the null-OPD point

Although the atmospheric differential piston is a random signal, its statistical properties are described by Tatarski's models. Let ΔL_{dp} be the OPD component related to the differential piston for an interferometer characterized by a projected baseline B and apertures of diameter equal to D. From Taylor's hypothesis of a frozen turbulence moving at velocity V_a (with $\mathbf{B} = k.\mathbf{V}_a$), the power spectrum of ΔL_{dp} can be modeled by[8]:

$$\begin{cases} \mathcal{W}_{\Delta L_{dp}}(f) \propto f^{-2/3} & ; \quad \text{if } f < \dfrac{\mathrm{V}_a}{2\mathrm{B}} \\ \mathcal{W}_{\Delta L_{dp}}(f) \propto f^{-8/3} & ; \quad \text{if } \dfrac{\mathrm{V}_a}{2\mathrm{B}} \leq f < \dfrac{0.3\mathrm{V}_a}{D} \\ \mathcal{W}_{\Delta L_{dp}}(f) \propto f^{-17/3} & ; \quad \text{if } f \geq \dfrac{0.3\mathrm{V}_a}{D} \end{cases} \tag{1}$$

This power spectrum indicates that the temporal autocorrelation of ΔL_{dp} is not equal to zero for $\tau \neq 0$ (τ being the argument of the autocorrelation function), i.e. ΔL_{dp} is not white-noise. We assume that only the atmospheric differential piston significantly modifies the position of the null-OPD point from one scan to the next one. The signal measured by the fringe-tracker is:

$$s[n] = \Delta L_{dp}[n] - \Delta L_{dp}[n-1] = \Delta L[n] - \Delta L_[n-1], \tag{2}$$

where n is an integer indexing the values of ΔL_{dp} for each scan. ΔL can be tracked from an origin by integrating s, yielding a temporal signal u. The fact that u, reflecting ΔL_{dp}, is temporally autocorrelated has been proved by using the first version of the fringe-tracker in open loop and measuring u for each scan from the position of the null-OPD point. The autocorrelation of u has then been computed yielding the result illustrated in Fig. 5. u can therefore be described by the auto-regressive (AR) model:

$$\tilde{u}[n+1] = \sum_{i=0}^{P-1} a[i].u[n-i], \tag{3}$$

where P is the order of the model. The issue is to determine the values of the AR model $\underline{a} = (a_0, ..., a_{P-1})^{\mathrm{T}}$ to minimize the mean quadratic error $< |u[n] - \tilde{u}[n]|^2 >$. Since no assumption regarding the stability of u can

be made, especially for long observing periods where the turbulence conditions are changing, one should use an adaptive method to correct the AR model at each step, according to the actual value of u (determinated from the algorithm described in part 2). We propose to use the weigthed recursive least square algorithm (WRLS), a familiar signal-processing method. At each scan indexed by n, the expected OPD is computed from the following equations:

$$\begin{cases} \underline{K}[n+1] = \underline{V}[n].\underline{u}[n].(\Lambda + \underline{u}[n]^{\mathrm{T}}.\underline{V}[n].\underline{u}[n])^{-1} \\ \underline{V}[n+1] = (\underline{1} - K[n+1].u[n]^{\mathrm{T}}).\underline{V}[n].\Lambda^{-1} \\ \underline{a}[n+1] = \underline{a}[n] + \underline{K}[n+1].(u[n+1] - \underline{a}[n]^{\mathrm{T}}.\underline{u}[n]) \end{cases} , \tag{4}$$

where $\underline{K}$ is a vector representing the adaptation gain (or "Kalman gain"), $\underline{V}$ is the covariance matrix, $\underline{1}$ is the identity matrix, $\underline{u}[n] = (u[n], ..., u[n-P-1])^{\mathrm{T}}$, and Λ is the "forgetting factor" used to accelerate the convergence of the AR model. Usually, $0.8 < \Lambda < 1$. This algorithm has already been proposed to improve fringe-tracking with GDT or RAFT[9]. Methods of the same type using ARMA models have been successfully used for adaptive optics[10]. In the case of IOTA, prediction could be employed for enhancing tip-tilt correction as well.

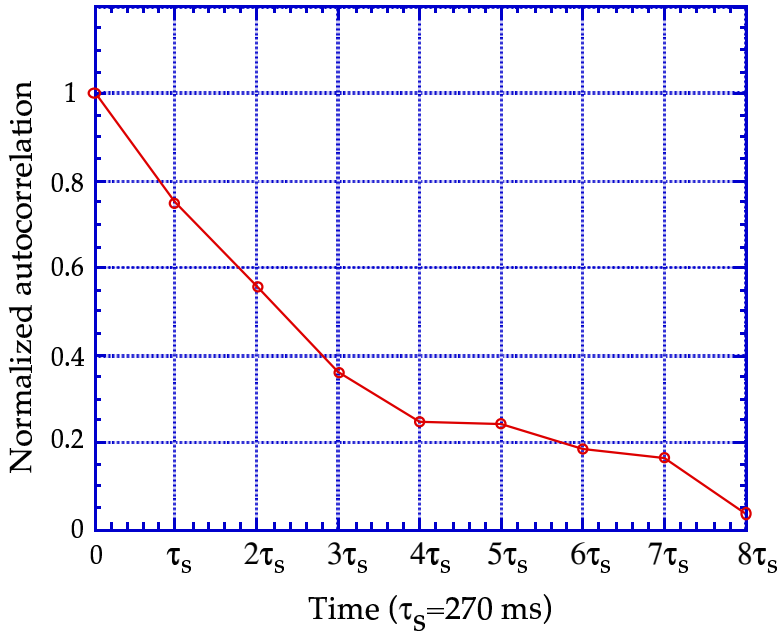

Figure 5. Normalized discrete temporal autocorrelation of the optical path difference drift (from a reference point) measured at IOTA with a 38 m baseline.

4.3 Fringe-tracking with FLUOR

The FLUOR recombiner has recently been improved and yields very accurate fringe contrast measurements. Its control system consists of a Macintosh G3 400 MHz computer in charge of NICMOS acquisition, scanning-PZT control (different from the one used on the beamsplitter table), and short-ODL control. The whole control software has been developed with National Instruments' LabVIEW graphic language. Thanks to this compact system and to the low scan rate used (2 Hz max.), a coherencer has easily been implemented on the FLUOR control system. It consists of finding the position of the centroid in the fringe packet. Each fringe packet has previously been filtered through a bandpass filter. Then, the mean of the raw fringe packet is added to the previous filtered signal to yield the final fringe packet to analyze. The OPD is corrected by moving the short-ODL. The FLUOR coherencer features an automatic fringe detector triggered when there is, in the interferogram, at least one peak whose amplitude is larger than a pre-set threshold. However, this detector may be deceived by "light-bursts", which sometimes occur in a fringe-packet. Detecting peaks at different bandwidths should eliminate this problem.

Since FLUOR is intended to be more heavily used on IOTA, it would be interesting to try to improve the FLUOR coherencer by using the algorithm described in part 2 and/or the prediction algorithm. Tests should be

carried out during year 2000. However, first tests of the coherencer algorithm applied to FLUOR have recently been done. For "clean" fringes with high SNR (obtained by observing π-Leo with the 38-meter baseline of IOTA) and good turbulence conditions, no significant difference between our algorithm and the centroid method appeared. In both cases, with a 2 Hz scan rate, the standard deviation of the residual OPD (difference between the measured null-OPD point and the center of the scan window) was $\sigma = 14\,\mu$m.

5. CONCLUSION

An automatic coherencing system for an infrared stellar interferometer can be made from a simple and fast algorithm. However, its implementation strongly depends on the characteristics of the existing control system. It is optimal to have only one computer in charge of fringe acquisition, null-OPD point measurement, and OPD correction. For IOTA, the current coherencer algorithm will normally used for the beamsplitter table during all observations once the new VxWorks system is installed. Then, prediction algorithms will be added to try to improve the performance of this coherencer. This might also benefit the FLUOR coherencer which already exists. New improved algorithms for measuring the null-OPD point in a fringe packet with a better accuracy are currently being studied. Closure-phase experiments at IOTA (scheduled for 2001) will certainly require such a coherencing system.

6. ACKNOWLEDGEMENTS

We thank M. G. Lacasse for his help during the fringe-tracker experiments at IOTA. We also thank V. Coudé du Foresto and G. Perrin for having helped us to use the FLUOR recombiner. S. Morel is grateful to DGA-DRET (the scientific research office of the French Ministry of Defense) which funded him in 1999, and to NASA and the Smithsonian Institution for his year 2000 fellowship.

7. REFERENCES

1. J. T. Armstrong, D. Mozurkewich, T. A. Pauls, A. R. Hajian, "Bootstrapping the NPOI: keeping long baselines in phase by tracking fringes on short baselines", *Proceedings SPIE, 'Astronomical Interferometry', 20-27 March 1998, Kona, Hawaii*, **3350**, pp. 461-466, 1998.
2. P. R. Lawson, "Group-delay tracking in optical stellar interferometry with the fast Fourier transform", *J. Opt. Soc. Am.* **A 12**, pp. 366-374, 1995.
3. L. Koechlin, P. R. Lawson, D. Mourard, A. Blazit, D. Bonneau, F. Morand, Ph. Stee, I.Tallon-Bosc, F.Vakili, "Dispersed fringe tracking with the multi-r_0 apertures of the Grand Interféromètre à 2 Télescopes", *Appl. Opt.* **35**, pp. 3002-3009, 1996.
4. M. Shao, D. H. Staelin, "Long-baseline optical interferometer for astrometry", *J. Opt. Soc. Am.* **67**, pp. 81-86, 1977.
5. V. Coudé du Foresto, G. Perrin, C. Ruilier, B. Mennesson, W. A. Traub, M. G. Lacasse, "FLUOR fibered instrument at the IOTA interferometer", *Proceedings SPIE, 'Astronomical Interferometry', 20-27 March 1998, Kona, Hawaii*, **3350**, pp. 856-863, 1999.
6. R. Millan-Gabet, F. P. Schloerb, W. A. Traub, N. P. Carleton, "A NICMOS3 camera for fringe detection at the IOTA interferometer", *Publ. Astron. Soc. Pac.* **111**, pp. 238-245, 1999.
7. W. A. Traub, N. P. Carleton, J. D. Bregman, M. K. Brewer, M. G. Lacasse, P. Maymounkov, R. Millan-Gabet, S. Morel, C. Papaliolios, M. R. Pearlman, I. Porro, F. P. Schloerb, "The third telescope project at the IOTA interferometer", *Proceedings SPIE, 'Interferometry in Optical Astronomy', 27-31 March 2000, Munich, Germany*, **4006**, in preparation.
8. G. Perrin, "Correction of the "piston effect" in optical astronomical interferometry. I. Modulus and phase gradient of the visibility function restoration", *Astron. & Astroph. Suppl. Ser.* **121**, pp. 553-568, 1997.
9. S. Morel, L. Koechlin, "Fringe tracking using a priori information on the optical path difference drift", *Proceedings SPIE, 'Astronomical Interferometry', 20-27 March 1998, Kona, Hawaii*, **3350**, pp. 1057-1064, 1998.
10. C. Dessenne, P.-Y. Madec, G. Rousset, "Optimization of a predictive controller for closed-loop adaptive optics", *Appl. Opt.* **37**, pp. 4623-4633, 1998.